

J. SCHUBERT^{1,✉}
O. TRITHAVEESAK¹
W. ZANDER¹
M. ROECKERATH¹
T. HEEG¹
H.Y. CHEN²
C.L. JIA²
P. MEUFFELS³
Y. JIA⁴
D.G. SCHLOM⁴

Characterization of epitaxial lanthanum lutetium oxide thin films prepared by pulsed-laser deposition

¹ Institute of Bio- and Nanosystems and Center of Nanoelectronic Systems for Information Technology, Research Centre Jülich, 52425 Jülich, Germany

² Institute of Solid State Research and Ernst Ruska-Centre for Microscopy and Spectroscopy with Electrons, Research Centre Jülich, 52425 Jülich, Germany

³ Institute of Solid State Research, Research Centre Jülich, 52425 Jülich, Germany

⁴ Department of Materials Science and Engineering, The Pennsylvania State University, University Park, PA 16802-5005, USA

Received: 23 August 2007/Accepted: 21 September 2007
Published online: 10 November 2007 • © Springer-Verlag 2007

ABSTRACT Epitaxial thin films of LaLuO₃ were deposited on SrTiO₃(100) and SrRuO₃/SrTiO₃(100) or SrRuO₃/LaAlO₃(100) substrates using pulsed-laser deposition. They were investigated by means of Rutherford backscattering spectrometry, X-ray diffraction, transmission electron microscopy and atomic force microscopy. Smooth, *c*-axis oriented films with a channeling minimum yield of 3% were obtained. The electrical characterization of Au/LaLuO₃/SrRuO₃/SrTiO₃(100) and Au/LaLuO₃/SrRuO₃/LaAlO₃(100) metal-insulator-metal capacitor stacks revealed a dielectric constant of $\kappa > 45$ and a breakdown field of 2 MV/cm for 100 nm thick epitaxial LaLuO₃ films.

PACS 73.61.Ng; 73.40.Rw; 77.22.Ch; 77.55.+f

1 Introduction

Many alternative gate oxides are being considered to replace silicon dioxide as the gate dielectric of future Si-based metal-oxide-semiconductor field-effect transistors (MOSFETs). For the moment HfO₂ is the favorite material with a dielectric constant $\kappa \approx 25$ and an optical bandgap of $E_g = 5.5$ eV. Hf-based oxide will be used in consumer electronics in the near future [1, 2]. One of the drawbacks of this material, however, is the low recrystallization temperature of amorphous HfO₂ films, ~ 600 °C [3]. Other materials being investigated include ternary rare earth scandate thin films [4] as well as binary rare earth oxides like La₂O₃ and Lu₂O₃, which can be grown by metal organic chemical vapor deposition, atomic layer deposition or molecular-beam epitaxy [5–7]. The dielectric constant of these binary oxides is around 15, which is too low compared to HfO₂, to be of interest. Schlom et al. proposed LaLuO₃ as a possible alternative gate oxide [2]. An optical bandgap of $E_g = 5.6$ eV and a κ -value of 22 was reported for a LaLuO₃ single crystal in a particular (undefined) direction [2]. Furthermore this material has a high melting temperature of 2120 °C and has been

proven to be stable against reduction when heated up in a vacuum or hydrogen atmosphere. Lopes et al. showed κ -values up to 32 and a bandgap of 5.2 eV for amorphous LaLuO₃ films grown by pulsed-laser deposition (PLD) [8]. All these characteristics are promising for the application of LaLuO₃ in a MOSFET structure. LaLuO₃ in its crystalline form has an orthorhombic crystal structure (*Pbnm* (62)) with lattice parameters of $a = 5.826$ Å, $b = 6.022$ Å, and $c = 8.38$ Å [9]. No literature with information about the growth and characterization of thin epitaxial LaLuO₃ films has been found.

2 Experimental

2.1 Thin film deposition

In this paper we discuss the properties of epitaxial LaLuO₃ films, which were deposited by PLD. An oxygen partial pressure of $(1\text{--}5) \times 10^{-3}$ mbar and a substrate temperature of 500 °C to 1000 °C were applied. A pellet made from a stoichiometric mixture of the metal oxides sintered at 1600 °C in air formed the target. SrTiO₃(100) was used as the substrate as well as epitaxially grown films of SrRuO₃ on SrTiO₃(100) or LaAlO₃(100). The epitaxial SrRuO₃ films comprised the bottom electrode of metal-insulator-metal (MIM) capacitors for the electrical characterization of the LaLuO₃ thin films and were grown with PLD as well.

The layers were investigated with respect to their morphology and chemical composition by means of Rutherford backscattering spectrometry (RBS), X-ray diffraction (XRD), and transmission electron microscopy (TEM). Parallel plate capacitors were formed by evaporation of ~ 100 nm thick gold films through a shadow mask. The capacitor stacks were investigated on a measuring station equipped with an impedance analyzer (HP 4192A) for recording of the *C*–*V* curves. The measurements were performed at a frequency of 10 kHz and 100 kHz. A dc voltage was applied to determine the breakdown field of the films.

2.2 Structural characterization

The stoichiometric transfer of LaLuO₃ from the target to the substrate was assessed by RBS and channeling provided the first check of the crystalline quality. Both

✉ Fax: +49-246-1614673, E-mail: j.schubert@fz-juelich.de

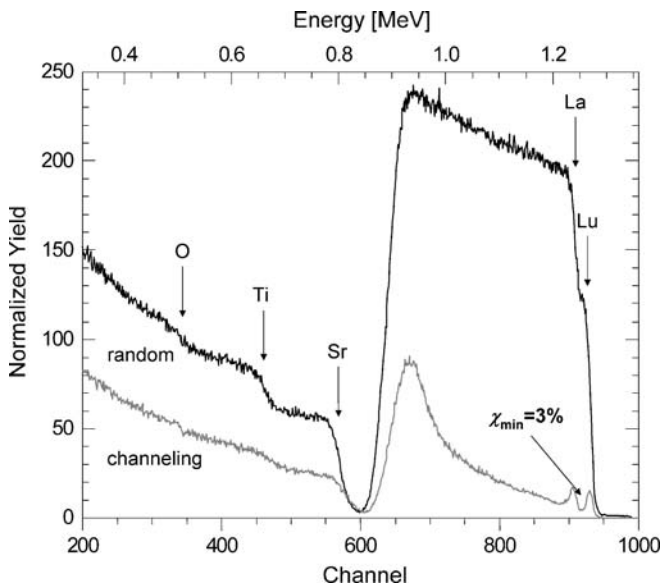


FIGURE 1 RBS-channeling measurement of a 360 nm thick LaLuO₃ film grown on SrTiO₃(100) at a substrate temperature of 900 °C. The positions of the different elements are marked by arrows. A minimum yield (χ_{\min}) of 3% confirms the good epitaxial growth of the layer

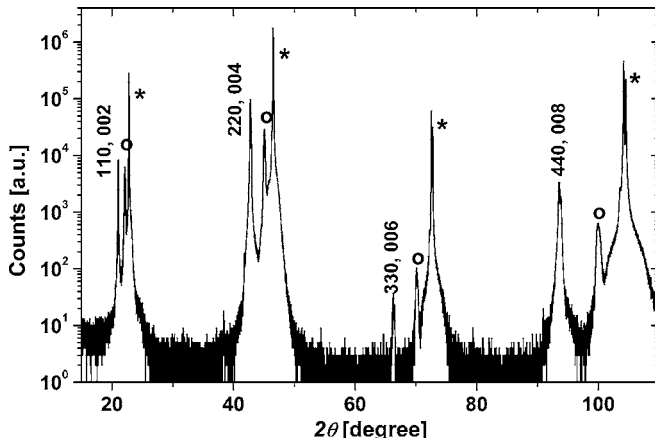


FIGURE 2 XRD measurement of a LaLuO₃ film grown on SrRuO₃/SrTiO₃(100) at a substrate temperature of 700 °C. Three sets of reflections are seen which belong to SrTiO₃ (*), SrRuO₃ (○), and LaLuO₃

results are seen in Fig. 1. A 360 nm thick film of LaLuO₃ grown at 900 °C on SrTiO₃(100) shows a stoichiometry which is close to the nominal composition of the target. The ratio La : Lu lies between 1 : 0.95 and 1 : 1.05. The minimum yield of $\chi_{\min} = 3\%$ reveals the good epitaxial growth of LaLuO₃ on SrTiO₃(100). Comparable results were obtained for films grown on epitaxial SrRuO₃ on SrTiO₃(100). In Fig. 2 a θ - 2θ XRD-measurement of a film grown on SrRuO₃/SrTiO₃(100) is displayed. In addition to the substrate peaks marked by asterisks and a set of peaks indexed by “o”, a third set of reflections arising from the LaLuO₃ film can be observed. The set indexed with “o” are from the epitaxial SrRuO₃ bottom electrode. Compared to the lattice parameter of bulk LaLuO₃ two possibilities exist for indexing the third set of peaks. They correspond to a lattice parameter of 4.21 Å. Multiplied by $\sqrt{2}$ this equals the *a*- or *b*-axis length of the LaLuO₃ single crystal and when multiplied by 2 the value is comparable to the *c*-axis of

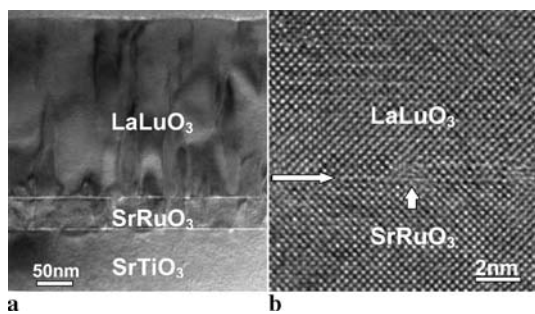


FIGURE 3 (a) TEM-micrograph of a 360 nm thick LaLuO₃ film grown on epitaxial SrRuO₃/SrTiO₃(100) at a substrate temperature of 700 °C (b) TEM-micrograph of the interface between LaLuO₃ and SrRuO₃. The perpendicular arrow marks a misfit dislocation at the interface of SrRuO₃ and LaLuO₃ (horizontal arrow)

the single crystal. TEM was used to investigate which orientation (*hh*0 or 0*0l*) is present in the samples.

The microstructure of the LaLuO₃ film grown on a SrRuO₃/SrTiO₃(100) substrate is shown in Fig. 3. The films of both SrRuO₃ and LaLuO₃ grow epitaxially on the SrTiO₃ substrate. In Fig. 3a, a low magnification micrograph gives an overview of the film morphology. The line contrast, white and black, in the film layers relates to the lattice defects. In the areas directly above the SrRuO₃/LaLuO₃ interface multidomains coexist with either the ⟨110⟩ or the ⟨001⟩ LaLuO₃ directions parallel to the normal of the film. With an increase of the film thickness, the ⟨001⟩ domains grow over the other domains, resulting in a pure *c*-axis orientation in the top part of the film. Misfit dislocations and stacking faults are observed at the interface. Figure 3b shows a lattice image of the interface between the SrRuO₃ layer and the LaLuO₃ layer. The interface is sharp (marked by arrows) and misfit dislocations are visible.

2.3 Electrical characterization

The electrical properties of the LaLuO₃ thin films were investigated by *C*-*V* measurements. The Au/LaLuO₃/

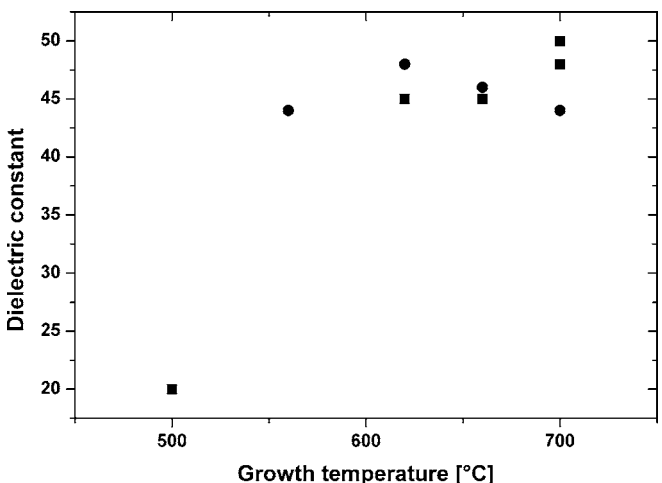


FIGURE 4 Dielectric constant values of Au/LaLuO₃/SrRuO₃/SrTiO₃(100) (■) and Au/LaLuO₃/SrRuO₃/LaAlO₃(100) (●) MIM capacitors grown at different substrate temperatures

SrRuO_3 MIM-capacitor stacks were prepared on samples grown at different temperatures on both $\text{SrTiO}_3(100)$ and $\text{LaAlO}_3(100)$ substrates. The results are summarized in Fig. 4. Films deposited at temperatures lower than 600°C were polycrystalline and had a κ of 20, comparable to the values measured on a single crystal. Samples grown at higher temperatures have a κ higher than 40. This number is much larger than the values published in [10]. In combination with the results obtained from the XRD- and TEM-measurements this value can be attributed to the permittivity of LaLuO_3 along the long axis, the [001] direction, for the $Pbnm$ setting of LaLuO_3 that we use in this manuscript. Breakdown voltage measurements on the samples resulted in a minimal value of 2 MV/cm measured on 80 nm thick films.

3 Summary

Epitaxial LaLuO_3 thin films prepared by PLD were grown on $\text{SrTiO}_3(100)$ as well as on $\text{SrRuO}_3/\text{SrTiO}_3(100)$ and $\text{SrRuO}_3/\text{LaAlO}_3(100)$. The layers possess the same stoichiometry as the target material and have low RBS channeling minimum yield values (3%). They are smooth and the crystalline orientation of films grown at temperatures higher than 600°C is (00l) perpendicular to the substrate surface. The κ value of 45, which is significantly higher than measured on single crystals, can be attributed to the anisotropy in the κ of LaLuO_3 . Here we measure the dielectric constant along the long axis in the orthorhombic LaLuO_3 crystal structure. A breakdown voltage of 2 MV/cm was measured on 80 nm

thin films. These results are promising for future high- κ applications of LaLuO_3 in MOSFETs.

ACKNOWLEDGEMENTS O.T. gratefully acknowledges the financial support by the Deutsche Forschungsgemeinschaft. M.R. gratefully acknowledges the financial support by the European network of excellence “SINANO”. T.H. gratefully acknowledges the financial support by the Deutsche Forschungsgemeinschaft (Graduiertenkolleg GRK 549 „Non-centrosymmetric Crystals“).

REFERENCES

- 1 http://www.intel.com/technology/silicon/45nm_technology.htm
- 2 D.G. Schlom, J.H. Haeni, MRS Bull. **27**, 198 (2002)
- 3 H. Kim, P.C. McIntyre, K.C. Saraswat, Appl. Phys. Lett. **82**, 106 (2003)
- 4 C. Zhao, T. Witters, B. Brijs, H. Bender, O. Richard, M. Caymax, T. Heeg, J. Schubert, V.V. Afanas'ev, A. Stesmans, D.G. Schlom, Appl. Phys. Lett. **86**, 132903 (2005)
- 5 G. Scarel, E. Bonera, C. Wiemer, G. Tallarida, S. Spiga, M. Fanciulli, I.L. Fedushkin, H. Schumann, Y. Lebedinskii, A. Zenkevich, Appl. Phys. Lett. **85**, 630 (2004)
- 6 S. Haukka, T. Suntola, Interface Sci. **75**, 119 (1997)
- 7 K. Kakushima, K. Tsutsui, S.I. Ohmi, P. Ahmet, V. Ramgopal Rao, H. Iwai, in *Topics in Applied Physics Vol. 106 “Rare Earth Oxide Thin Films”*, ISBN 3-540-35796-3 (Springer, Heidelberg, 2006), pp. 115–126
- 8 J.M.J. Lopes, M. Roeckerath, T. Heeg, E. Rije, J. Schubert, S. Mantl, V.V. Afanas'ev, S. Shamuilia, A. Stesmans, Y. Jia, D.G. Schlom, Appl. Phys. Lett. **89**, 222902 (2006)
- 9 K.L. Ovanesyan, A.G. Petrosyan, G.O. Shirinyan, C. Pedrini, L. Zhang, Opt. Mater. **10**, 291 (1998)
- 10 D.G. Schlom, C.A. Billman, J.H. Haeni, J. Lettieri, P.H. Tan, R.R.M. Held, S. Völk, K.J. Hubbard, in *Thin Films and Heterostructures for Oxide Electronics*, ed. by S.B. Ogale (Springer, New York, 2005), pp. 31–78